Honeycomb Networks and Chiral Superstructures Formed by Cyanuric Acid and Melamine on Au(111)

P. A. Staniec,[†] L. M. A. Perdigão,[†] B. L. Rogers,[†] N. R. Champness,[‡] and P. H. Beton*[,†]

School of Physics & Astronomy, University of Nottingham, Nottingham, NG7 2RD, U.K., and School of Chemistry, University of Nottingham, Nottingham, NG7 2RD, U.K.

Received: August 2, 2006; In Final Form: October 25, 2006

Two distinct bimolecular cyanuric acid−melamine intermixed structures, a honeycomb network and a larger superstructure, have been observed on Au(111) using a scanning tunneling microscope under ultrahigh vacuum conditions. The superstructure is formed as a regular array of chiral hexagonal rings of melamine, linked by single molecules of cyanuric acid. These bimolecular networks show both key similarities and differences to related networks studied previously on surfaces and in bulk phases. We also compare our results with networks formed by related molecules on Au(111) and Ag-terminated silicon.

Introduction

The formation of 2D arrays of nanostructures through the selective use of highly directional noncovalent interactions is currently of significant interest. Such interactions have been exploited widely in solution-based chemistry to direct the assembly of molecules into nanometer-sized functional structures.[1−3] More recently, these concepts have been applied to the formation of self-assembled nanostructures at surfaces.[4−27] This approach has great potential, for example, in the creation of functionalized surfaces via the spontaneous association of the molecular components under equilibrium conditions. Structures so formed can have dimensions smaller than those attainable with conventional processing techniques such as electron-beam lithography. In particular, hydrogen bonds[28] have been shown to stabilize a wide range of structures from clusters[6−8] and rows[8−12] to more complicated open structures.[7,13−20]

We have demonstrated previously that a bimolecular honeycomb array of PTCDI and melamine molecules, stabilized by hydrogen bonds, may be formed both on a passivated semiconductor surface[18] and a metallic gold surface[19] with relatively minor changes in the preparation conditions. This honeycomb array was shown to form a template for adsorption of further molecular species. We now report investigations into varying the molecular components in order to gain insight into the possible control over the resulting structures and their properties, which will ultimately lead to design rules for such structures.

Recently, we have published a study of the bimolecular network formed between cyanuric acid and melamine on the Ag-Si(111)-($\sqrt{3} \times \sqrt{3}$)R30° surface.[20] Cyanuric acid and melamine were shown to form a single honeycomb structure, consisting of various domains. The interaction between cyanuric acid and melamine has long been studied and exploited in supramolecular chemistry,[29−38] and the array formed in the bulk shows a close similarity with that observed on the Ag-terminated Si surface.

In this paper, we show that the cyanuric acid−melamine (CA·M) bimolecular array may also be formed on the metallic Au(111) substrate. However, on the Au(111) surface two distinct structures are observed. The first is a honeycomb structure similar to that reported on the Ag-Si(111)-($\sqrt{3} \times \sqrt{3}$)R30° surface. The second is a chiral superstructure, which appears to have a higher degree of long-range ordering.

Experimental and Theoretical Methods. A Au(111) surface was prepared by loading a 5 mm × 10 mm piece of gold on mica (purchased from Molecular Imaging Inc.) into an ultrahigh vacuum (UHV) system with a base pressure of 1×10^{-10} Torr. The surface was cleaned using Ar ion sputtering (4×10^{-6} Torr, 1 kV, 1−3 μA) followed by annealing at 150−450 °C for several hours. Images of the surface were acquired using a scanning tunneling microscope (STM) housed within the UHV system, using electrochemically etched tungsten tips and operating in constant-current mode at room temperature. Following the sputter-anneal cycle, we observed the characteristic ($22 \times \sqrt{3}$) herringbone reconstruction of the Au(111) surface.[39] Cyanuric acid and melamine were sublimed onto the gold surface, which was held at room temperature, by heating charges of the materials in Knudsen cells to ∼160 °C and ∼140 °C, respectively.

Experimental results have been supported by density functional theory (DFT) calculations performed using the SIESTA package.[40,41] Following the approach used in our previous work,[23] the linear combination of atomic orbitals (LCAO) and the Perdew−Burke−Enzerhof[42] generalized gradient approximations were used. The results of several previous studies provide adequate post-hoc evidence of the efficacy of this approach to the simulation of hydrogen-bonded molecular networks.[43,44] Core electrons were represented by pseudopotentials constructed according to the method described by Troullier and Martins,[45] while double-ζ basis sets with polarization functions were used to describe the valence electrons. The radius within which the atomic orbitals are strictly localized is defined in the SIESTA code by the energy shift, which in our calculations was set to 0.5 mRy. The default convergence tolerance of 10^{-4} eV was employed for the self-consistent field (SCF) cycle at each stage of the optimization. Geometry optimization was performed using the conjugate gradient method with a convergence force tolerance of 0.01 eV Å^{-1}. The calculated binding energies were corrected for the basis set

* Corresponding author. Tel: +44 (0) 115 9515129. Fax: +44 (0) 115 951 5180. E-mail: Peter.Beton@nottingham.ac.uk.
† School of Physics & Astronomy.
‡ School of Chemistry.

10.1021/jp064964+ CCC: $37.00
Published on Web 12/14/2006

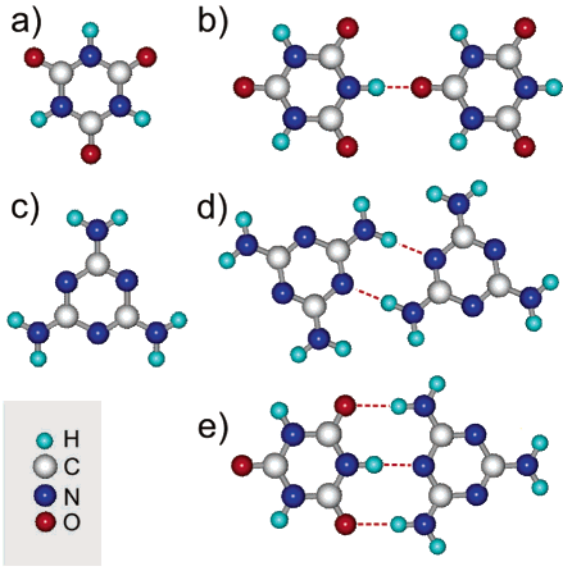

Figure 1. (a) Molecular structure of cyanuric acid; (b) the single hydrogen bond, identified by a red dotted line, between a pair of cyanuric acid molecules; (c) molecular structure of melamine; (d) the double hydrogen bond between a pair of melamine molecules; (e) the triple hydrogen bond between a cyanuric acid molecule and a melamine molecule.

superposition error (BSSE) according to the counterpoise method described by Boys and Bernardi.[46] Our calculations were aimed at determining the molecular dimensions and binding energies of the gas-phase hydrogen-bonded pairs of molecules. The Au(111) surface was not included in the calculations.

Results

Cyanuric Acid. Between 0.1−0.3 monolayers of cyanuric acid (Figure 1a) were deposited onto a freshly prepared Au(111) surface. Figure 2a shows an STM image of one of the resulting large hexagonally ordered islands. The average center−center molecular spacing, d, is measured to be 6.95 ± 0.25 Å, with the cyanuric acid rows running at an angle of 4.2° ± 1.0° relative to the $\langle 11\bar{2}\rangle$ directions. In the case of all systems reported here, the underlying herringbone reconstruction of the Au(111) was observed beneath the adsorbed materials. This continuation of the reconstruction underneath the adsorbed molecular islands is indicative of a weak molecule−substrate interaction.[21]

We propose a model (Figure 2b) for the observed molecular ordering in which each cyanuric acid molecule forms a single hydrogen bond (see Figure 1b) with each of its six neighbors. DFT calculations performed on a model cluster of three cyanuric acid molecules in a triangular configuration, equivalent to the proposed adlayer arrangement (see Figure 2c), yield a center−center separation of d = 6.80 Å, consistent with our experimentally measured values.

We further propose a model for the adsorption of molecules on the Au(111) surface. As discussed by Barth et al.,[21,39] upon reconstruction Au(111) is no longer perfectly hexagonal but becomes locally contracted along a $\langle 1\bar{1}0\rangle$ direction (perpendicular to $\langle 11\bar{2}\rangle$). Here, we treat the Au(111) surface reconstruction as a 4.55% homogeneous compression realized perpendicular to the single $[11\bar{2}]$ direction shown in Figure 2b and neglect the small variation of interatomic separations within the true $(22 \times \sqrt{3})$ unit cell of the reconstructed surface.[39] This results in a constant interatomic distance along the contraction direction of a_3 = 2.75 Å while the other two interatomic

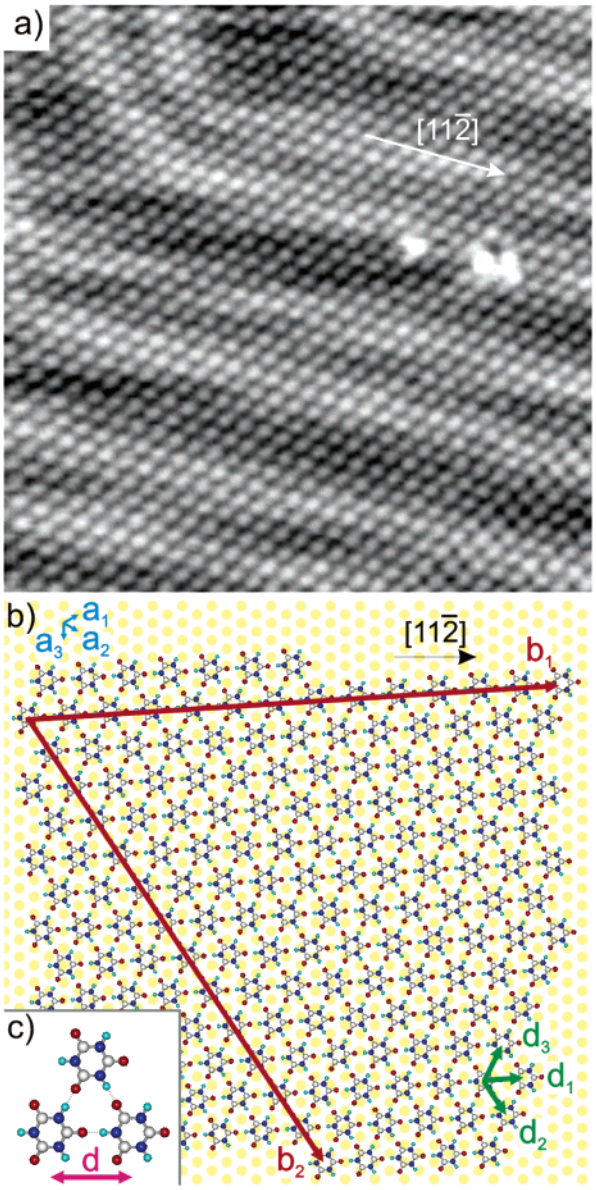

Figure 2. (a) STM image of hexagonally ordered island of cyanuric acid on Au(111), 185 Å × 185 Å, −2.3 V, 0.03 nA; the $[11\bar{2}]$ direction of the Au(111), taken from the herringbone reconstruction, is identified; (b) schematic of the proposed cyanuric acid overlayer on the reconstructed Au(111) surface, represented as yellow dots; the unit cell vectors $\mathbf{b_1}$ and $\mathbf{b_2}$ are shown by red arrows; the reconstructed Au(111) lattice vectors, $\mathbf{a_1}$ and $\mathbf{a_2}$, along with their linear combination, $\mathbf{a_3}$, are shown by blue arrows; the cyanuric acid molecular center−center separation in the three directions, d_1, d_2, and d_3, are shown by green arrows; (c) trimer arrangement of cyanuric acid used in DFT calculations to obtain the center−center separation, d, shown.

distances, a_1 and a_2, are taken to be 2.85 Å. In our following discussion $\mathbf{a_1}$ and $\mathbf{a_2}$ are taken as the unit cell vectors of the reconstructed surface. All matrix notation reported below is referenced to these vectors.

In developing a model for adsorption for cyanuric acid (and also the cyanuric acid-melamine complex, see below) we highlight the fixed angle observed between the principal axes of the hexagonal molecular overlayer and the underlying Au surface. In the light of the nonrandom orientation of the overlayer, we consider models that result in a coincidence lattice with long-range commensurability which give a misorientation angle and intermolecular spacing consistent with our measured and calculated values. The model is shown in Figure 2b. Vectors $\mathbf{b_1}$ and $\mathbf{b_2}$ are the unit cell vectors of the commensurate structure.

TABLE 1: Cyanuric Acid Center−Center Molecular Separations[a]

	d_1	d_2	d_3
measured on Au(111)		6.93 ± 0.25 Å	
DFT calculation		6.80 Å	
model for adsorption	6.93 Å	6.72 Å	6.69 Å

[a] Comparison of the cyanuric acid center−center separations, *d*, along the three principal axes (as shown in Figure 2b) between measured and calculated values.

The large length of these vectors relative to the molecular arrangement is justified from the observation in Figure 2a that the cyanuric acid domain forms a small angle relative to the [11$\bar{2}$] direction of the Au(111) surface. Each unit cell contains 169 cyanuric acid molecules. The intermolecular separations of cyanuric acid within this model, d_1, d_2, and d_3, are defined in Figure 2b, and values are given in Table 1, together with a comparison with measured and experimental values.

With reference to the reconstructed Au(111) surface, the commensurate structure can be described in matrix notation as

$$\begin{pmatrix} 20 & 16 \\ -16 & 36 \end{pmatrix}$$

Because the hexagonal structure is irregular, the center−center molecular separations d_1, d_2, and d_3 are inequivalent, ranging from 6.69 to 6.93 Å, as summarized in Table 1. The principal axis of the structure is rotated by 3.67° to the [11$\bar{2}$] direction.

The intermolecular spacings determined in our model are within approximately 0.1 Å of the calculated equilibrium gas-phase value and in agreement with our measured value. A hexagonally arranged structure of cyanuric acid has been observed previously on the Ag-Si(111)-($\sqrt{3} \times \sqrt{3}$)R30° surface[20] and measured to have a molecular spacing of 6.65 Å. This is comparable with the molecular spacings of 6.69 Å and 6.72 Å (see Table 1) and substantiates the use of these values in our model. The bulk structure for cyanuric acid, determined via X-ray crystallography,[47] is not hexagonal and, therefore, the dimensions are not comparable.

Because of the comparative inflexibility of the cyanuric acid molecules, a strain is placed on the hydrogen-bond lengths by the irregular geometry. This "flexible" behavior of hydrogen-bonded molecular adlayers with regard to the Au(111) reconstruction has been studied previously.[21] Our DFT calculations of the gas-phase geometry predict the N−H···O═C hydrogen bond to be 1.72 Å long. Assuming the molecules undergo minimal distortion upon adsorption, the variation of ±0.1 Å in our model represents a ∼6% change in the hydrogen bond length. Such distortions of gas-phase hydrogen-bond lengths upon adsorption to a surface have been reported previously.[5,22]

In principle, it is also possible for cyanuric acid to interact via the formation of pairs of hydrogen bonds,[47] similar to the surface behavior observed for PTCDI and related molecules.[9,13,18] This would lead to a honeycomb arrangement and is not in agreement with our observations of a hexagonal array. We have estimated the gas-phase binding energy between a pair of cyanuric acid molecules bonding via a single hydrogen bond (as arranged in our proposed structure) and via a double hydrogen bond. These yield a stabilization energy of −0.12 eV for a single hydrogen-bond arrangement and −0.18 eV for the double hydrogen-bond interaction. In a hexagonal close-packed arrangement, each cyanuric acid molecule forms a single hydrogen bond with six neighboring molecules, as opposed to three double hydrogen bonds with neighbors in a honeycomb arrangement. Therefore, we can estimate the stabilization energy per molecule in a hexagonal close-packed arrangement to be approximately −0.36 eV compared to −0.27 eV for a theoretical honeycomb arrangement, suggesting that the latter does not occur because it is energetically unfavorable.

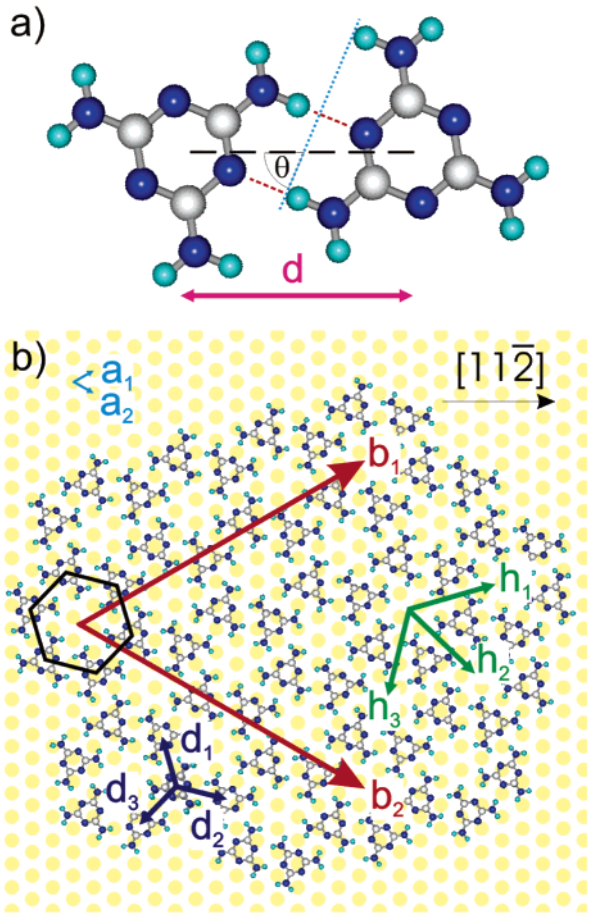

Figure 3. (a) A pair of melamine molecules as used in DFT calculations to obtain the center−center separation, *d*; due to the double hydrogen bonds, the molecular edge is rotated by an angle of θ to the line connecting the melamine centers; (b) schematic of the proposed arrangement of the melamine overlayer on the reconstructed Au(111) surface; the unit cell vectors $\mathbf{b_1}$ and $\mathbf{b_2}$ are shown by red arrows; the honeycomb period in the three directions, h_1, h_2, and h_3, are shown by green arrows; a hexagon highlights a melamine ring; the melamine center−center intermolecular separation in the three directions, d_1, d_2, and d_3, are shown by dark blue arrows; the reconstructed Au(111) lattice vectors, $\mathbf{a_1}$ and $\mathbf{a_2}$, are shown by blue arrows.

Melamine. We have shown previously[19] that melamine (Figure 1c) forms ordered honeycomb arrays on the Au(111) surface, measured to have an average period of 10.9 ± 0.2 Å. In more recent studies, through the acquisition of images of the substrate surface with atomic resolution, we have been able to establish a model for adsorption on the Au(111) surface and we include this below so it can be explicitly compared to the cyanuric acid and melamine mixtures. In these previous studies, melamine is stabilized by a double hydrogen bond (Figure 1d) similar to that observed in bulk melamine.[48] These two hydrogen bonds are not centered along the molecular edge (Figure 3a) and consequently the direction of the double hydrogen bonds between a pair of melamine molecules is not parallel to the line connecting their centers. Instead, the melamine molecular edges are rotated by an angle, θ, with respect to the line connecting their centers. The resulting melamine pair, therefore, gives rise to a chiral hexagonal arrangement. By placing these melamine pairs on a hexagonal lattice, an extended honeycomb arrangement is formed, shown in Figure 3b. DFT calculations

TABLE 2: Melamine Ring Period Lengths and Center−Center Intermolecular Separations[a]

	h_1	h_2	h_3	d_1	d_2	d_3
measured	10.9 ± 0.2 Å			6.3 ± 0.1 Å [b]		
DFT calculation	10.53 Å			6.08 Å		
model for adsorption	11.17 Å	10.97 Å	10.74 Å	6.21 Å	6.45 Å	6.34 Å

[a] Comparison of the hexagonal melamine array period, *h*, along their corresponding three principal axes and of the center−center intermolecular separations, *d*, (as shown in Figure 2b) between measured and calculated values. [b] Value derived from measured pore separation.

performed[19] on a single pair of melamine molecules predict a center−center separation of $d = 6.08$ Å with $\theta = 67°$. From this calculated separation, the period of the melamine array is estimated to be $\sqrt{3}d = 10.53$ Å.

In the proposed model, Figure 3b, vectors $\mathbf{b_1}$ and $\mathbf{b_2}$ are the unit cell vectors of the commensurate structure. With reference to the reconstructed Au(111) surface, the commensurate structure can be described in matrix notation as

$$\begin{pmatrix} 14 & 0 \\ 0 & 14 \end{pmatrix}$$

According to our model, the honeycomb arrays are irregular. The period of the melamine rings (parameters h_1, h_2 and h_3 as defined in Figure 3b) range from 10.74 to 11.17 Å, with a mean value of 10.97 Å in good agreement with our images. The melamine intermolecular separations range from 6.21 to 6.45 Å. These values are summarized in Table 2. Assuming that the melamine molecules do not undergo distortion upon adsorption to the surface, this represents a 19% increase in the hydrogen-bond lengths compared to the calculated gas-phase values. This compares with a distortion of ~20% for a hydrogen-bonded system reported previously on the Au(111) surface.[21]

Cyanuric Acid·Melamine. When cyanuric acid and melamine are combined on the surface, we see no evidence of the pure cyanuric acid or melamine phases described above. Rather, we observe two distinct intermixed phases of cyanuric acid and melamine (CA·M). Figure 4a shows an STM image of the two structures adjacent on the surface. The first structure, highlighted in the area marked α, is a honeycomb structure similar to that reported recently on the Ag-Si(111)-($\sqrt{3} \times \sqrt{3}$)R30° surface[20] and to the rosette structures reported in earlier studies of bulk CA·M.[29,31−35] In these structures (see Figure 5) cyanuric acid−melamine pairs are stabilized by triple hydrogen bonds (see Figure 1e), forming hexagons containing three cyanuric acid and three melamine molecules. The structure labeled area β in Figure 4a will be discussed later. Area γ is composed of small honeycomb domains with different orientations. These small domains have been observed extending over large areas. They are characterized by quasi-continuous variations in the local ordering rather than abrupt changes at boundaries (see Figure 4b). This behavior is comparable with that observed on the Ag-Si(111)-($\sqrt{3} \times \sqrt{3}$)R30° surface.[20] In some cases the variation is on a length scale comparable with the period of the honeycomb network. Because of the small size and the quasi-continuous nature of many of the domains, the dimensions and orientations with respect to the substrate cannot be readily identified (see Figure 4b). In addition, this observation implies that the stabilization due to the molecule−substrate interaction is moderately weak.

Despite these areas of local ordering, we observed that the orientation of the honeycomb network indicated in area α (Figure 4a) is more prevalent, forming over a range of approximately 10 unit cells, and as such, its orientation can be

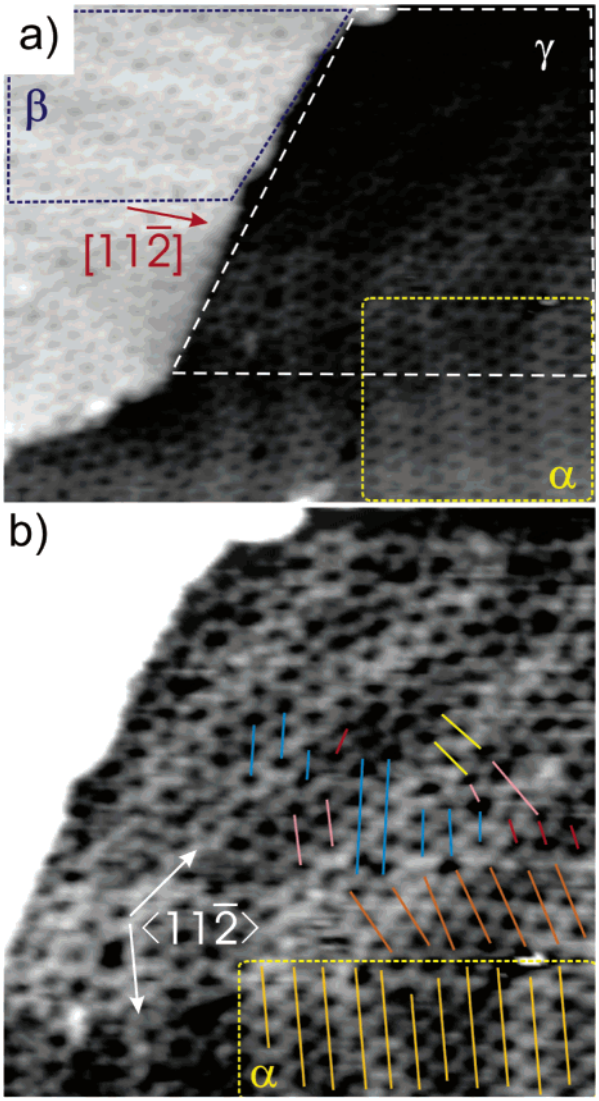

Figure 4. (a) STM image showing two distinct adjacent structures formed between cyanuric acid and melamine molecules on Au(111), 224 Å × 190 Å, −0.4 V, 0.03 nA; the [11$\bar{2}$] direction of the Au(111), taken from the herringbone reconstruction, is identified; area α shows an ordered structure of honeycomb CA·M networks, following the [11$\bar{2}$] of the Au(111) surface; area β shows an area of the larger chiral CA·M superstructure; area γ shows an area of honeycomb networks composed of several small domains and quasi-continuous variations in local ordering; this area (148 Å × 148 Å) is enlarged in part b with several domain directions highlighted.

deduced. The principal axis of this honeycomb domain is parallel to the [11$\bar{2}$] direction of the Au(111) surface (see Figure 5a).

We propose a model, Figure 5b, based on this alignment. The unit cell vectors, $\mathbf{b_1}$ and $\mathbf{b_2}$, along with their linear combination, $\mathbf{b_3}$, follow the circular pore directions. With reference to the reconstructed Au(111) surface, the commensurate structure can be described in matrix notation as

$$\begin{pmatrix} 2 & 2 \\ -2 & 4 \end{pmatrix}$$

The distorted honeycomb network has a period of 9.99 Å and 9.65 Å along $\mathbf{b_1}$ and $\mathbf{b_2}$, respectively. Within this model, the cyanuric acid and melamine center−center separation ranges from 5.51 to 5.77 Å.

In DFT calculations carried out using a model cluster of three melamine molecules bound to a single cyanuric acid molecule (see Figure 5c), the center−center separation of melamine and

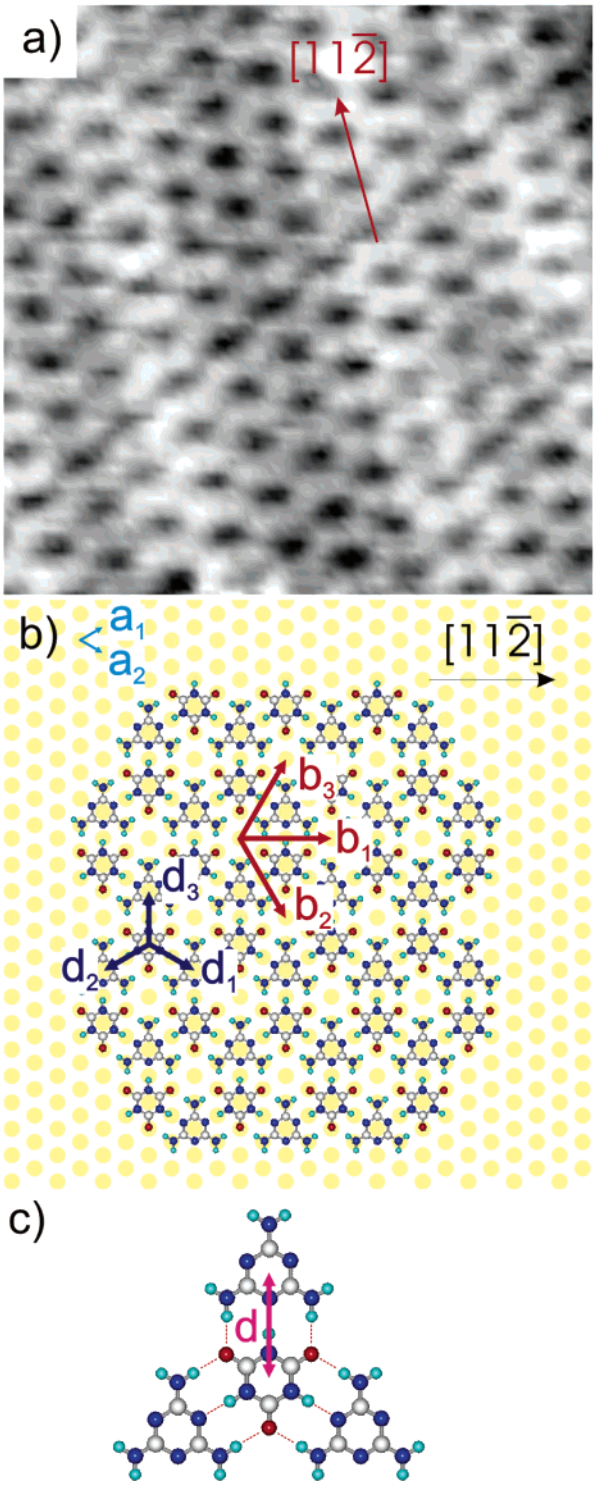

Figure 5. (a) STM image of the CA·M honeycomb network domain following the [11$\bar{2}$] direction of the Au(111), 80 Å × 80 Å, −0.4 V, 0.03 nA; the [11$\bar{2}$] direction of the Au(111) is labeled; (b) schematic of the CA·M honeycomb network on the reconstructed Au(111) surface; the unit cell vectors, $\mathbf{b_1}$ and $\mathbf{b_2}$, along with their linear combination, $\mathbf{b_3}$, are shown by red arrows; the cyanuric acid−melamine center−center molecular separation in the three directions, d_1, d_2 and d_3, are shown by dark blue arrows; the reconstructed Au(111) lattice vectors, $\mathbf{a_1}$ and $\mathbf{a_2}$, are shown by blue arrows; (c) the arrangement of three melamine molecules bonded to a single central cyanuric acid molecule used in DFT calculations to obtain the center−center separation, d.

cyanuric acid was found to be 5.46 Å, inferring a hexagonal array with a period of 9.46 Å. From X-ray diffraction studies, the lattice constant for bulk CA·M has been determined as 9.641 Å,[49] corresponding to a center−center separation of melamine and cyanuric acid of 5.55 Å. These values are compared in Table 3. The 9.99−9.65 Å period range is consistent with honeycomb periods of domains that have been reported on the Ag-Si(111)-($\sqrt{3} \times \sqrt{3}$)R30° surface,[20] with lattice periods ranging from 9.60 Å to 10.16 Å. The 9.65 Å value is very close to bulk values taken from X-ray crystallography and our DFT calculated value.

TABLE 3: CA·M Center−Center Separation and Honeycomb Periods[a]

	$\mathbf{b_1}$	$\mathbf{b_2}$	$\mathbf{b_3}$	$\mathbf{d_1}$	$\mathbf{d_2}$	$\mathbf{d_3}$
X-ray diffraction[49]		9.64 Å			5.55 Å	
DFT calculation		9.41 Å			5.43 Å	
adsorption model	9.99 Å	9.65 Å	9.65 Å	5.70 Å	5.70 Å	5.51 Å

[a] Table comparing the CA·M center−center separations, d, along the three principal axes (as shown in Figure 5b) for our commensurate model, gas-phase DFT calculations and from bulk studies using X-ray crystallography.[49] The corresponding values for the hexagonal honeycomb period are shown.

We draw attention to the fact that this particular domain results in all of the constituent molecules within the network being adsorbed at identical bonding sites (Figure 5b). In this configuration, it is possible for all molecules to be adsorbed in the most energetically favorable site and may offer an explanation as to why this domain appears more abundantly and over longer ranges than other honeycomb domains.

The second structure we observe, highlighted area β in Figure 4a, is a chiral structure with a larger unit cell (Figure 6a). This superstructure adopts a single orientation with respect to the herringbone reconstruction and has more extended long-range order. The superstructure gives rise to two distinct features in an STM image; a hexagonal arrangement of circular depressions, each surrounded by six elliptical features.

A model for this arrangement is proposed in which hexagonal rings of melamine molecules are interlinked by cyanuric acid molecules, as shown in Figure 6b. We note that the melamine/cyanuric acid ratio in this structure is 3:1, whereas in the previous structure the ratio is 1:1. Because of the chirality of the melamine rings, this new superstructure adopts a chiral arrangement. The cyanuric acid molecules, highlighted in Figure 6a, serve to illustrate the chirality of the melamine rings in a similar fashion to that reported previously in an intermixed melamine/PTCDI phase on the Au(111) surface.[19]

The formation of the superstructure can be illustrated as follows. Each melamine molecule within the melamine−melamine (M·M) hexagonal ring (see Figure 7a) is bonded to two other melamine molecules, and to one cyanuric acid molecule by a triple hydrogen bond (see Figure 1e). Each of the cyanuric acid molecules can then interact with two additional melamine molecules within other hexagonal rings (see Figure 7b). As a result, the cyanuric acid molecules bind an array of melamine hexagonal rings together to form the long-range ordered superstructure. This superstructure is expected to generate the two distinct features, hexagonal and elliptical, observed in STM images (see Figure 7c); the larger symmetrical depression is attributed to the center of the melamine rings and the elongated features to the elliptical linking structures formed between four melamine and two cyanuric acid molecules. The arrangement of these elliptical structures highlights the chirality of the overall arrangement. We draw attention to the fact that the hexagonal structure of the melamine rings is not aligned to that of the overall hexagonal superstructure.

From our observation that this superstructure has principal axes that are parallel to those of the Au(111) surface, we propose a model for adsorption that is shown in Figure 6b. The

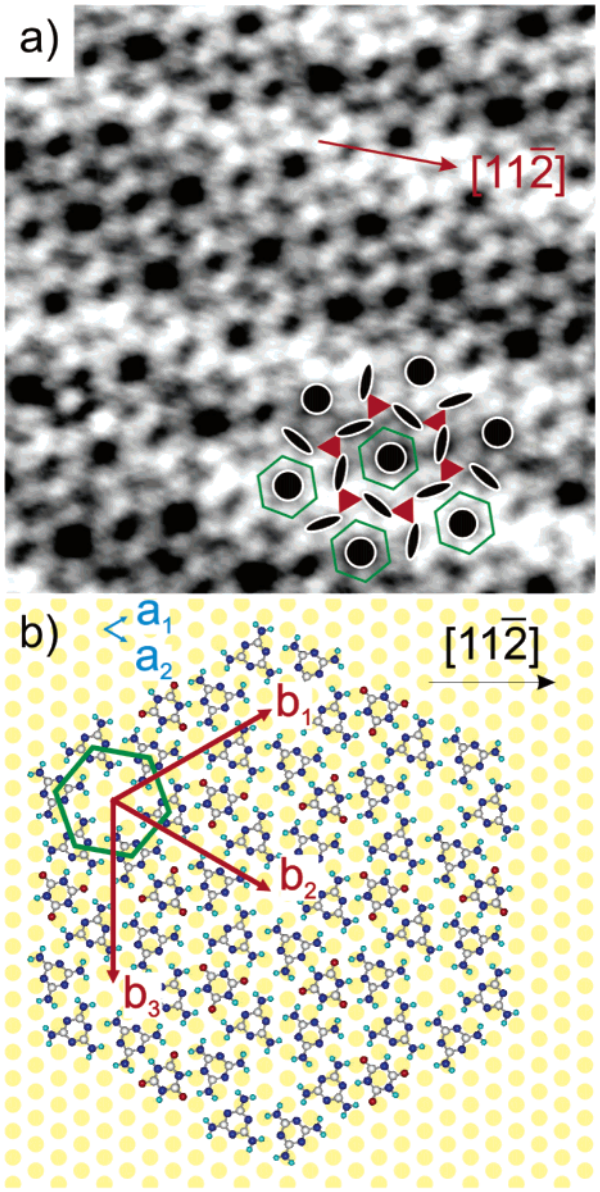

Figure 6. (a) STM image of the chiral CA·M superstructure on the Au(111), 100 Å × 100 Å, −1.2 V, 0.05 nA; the [11$\bar{2}$] direction of the Au(111) is labeled; the pattern formed by the structure is highlighted in the bottom-right corner; melamine rings and cyanuric acid molecules are highlighted schematically by green hexagons and red triangles, respectively; (b) schematic of the CA·M superstructure on the reconstructed Au(111) surface; the unit cell vectors, $\mathbf{b_1}$ and $\mathbf{b_2}$, along with their linear combination, $\mathbf{b_3}$, are shown by red arrows; the reconstructed Au(111) lattice vectors, $\mathbf{a_1}$ and $\mathbf{a_2}$, are shown by blue arrows; one melamine hexagonal ring is highlighted; note that because of the rotation of the melamine molecules with respect to the line connecting their centers, the melamine hexagonal ring is not aligned to the overall hexagonal lattice.

superstructure, with reference to the reconstructed Au(111) surface, can be described in matrix notation as

$$\begin{pmatrix} 7 & 0 \\ 0 & 7 \end{pmatrix}$$

The unit cell vectors, $\mathbf{b_1}$ and $\mathbf{b_2}$, along with their linear combination, $\mathbf{b_3}$, are defined on Figure 6b, and follow the circular pore directions. The overall hexagonal structure is irregular, with predicted pore separations of 19.98 Å along $\mathbf{b_1}$ and $\mathbf{b_2}$, and 19.32 Å along $\mathbf{b_3}$ (see Table 4).

Using the DFT calculated values of melamine−melamine and melamine−cyanuric acid center−center separation that were

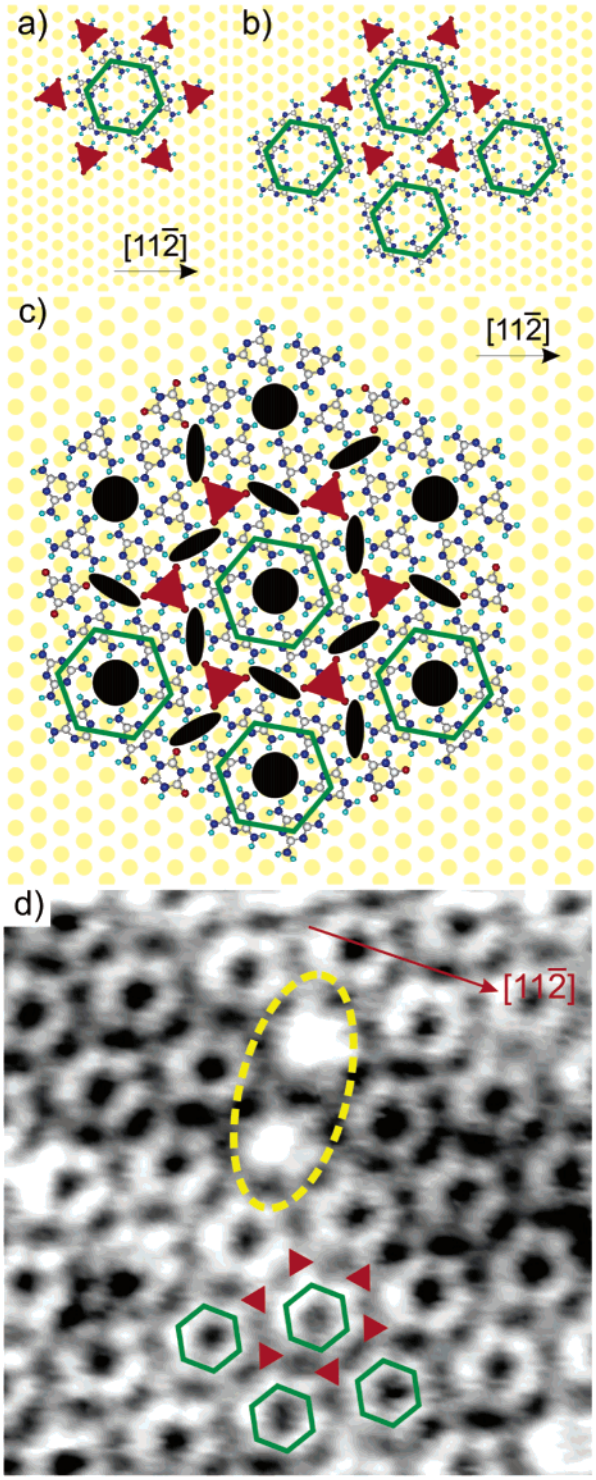

Figure 7. Illustration of the superstructure formation with (a) one melamine ring surrounded by six cyanuric acid molecules and (b) three melamine rings added to the previous ring, interlinked by four of the cyanuric acid molecules; (c) illustration of the chiral pattern formed by the superstructure shown against the model; (d) additional STM image of the superstructure following a tip change, possibly due to transfer of material from the surface; melamine rings and cyanuric acid molecules are highlighted schematically; two melamine rings, circled, appear to have adsorbed material in their centers.

discussed above, we predict a regular hexagonal superstructure with a period of 19.56 Å. We note that while this is very close to the mean value for b_1, b_2, and b_3, $\bar{b} = 19.65$ Å, the variation around this mean is up to 0.42 Å. We point out that this strain is spread over four hydrogen-bonded junctions.

TABLE 4: CA·M Superstructure Unit Cell Lengths[a]

	$\mathbf{b}_1$	$\mathbf{b}_2$	$\mathbf{b}_3$
DFT calculations		19.56 Å	
adsorption model	19.98 Å	19.98 Å	19.32 Å

[a] Comparison of values for the CA·M unit cell lengths, $\mathbf{b}_1$ and $\mathbf{b}_2$, along with their linear combination, $\mathbf{b}_3$, (as shown in Figure 6b) between calculated and model values.

We have estimated the gas-phase binding energy between a pair of melamine molecules (Figure 1d) and between a cyanuric acid and melamine molecule (Figure 1e) to be −0.44 eV and −0.79 eV, respectively. In the smaller honeycomb structure this results in an average stabilization energy per molecule of −1.19 eV, compared to −0.92 eV in the larger superstructure. This is as expected because the average number of hydrogen bonds per molecule is greater in the honeycomb structure than in the superstructure. Therefore, we tentatively propose that the honeycomb networks are an energetically favorable arrangement but that the larger superstructure forms due to a local stoichiometric excess of melamine molecules.

A different contrast of the superstructure has been observed in instances when the tip has undergone a change, probably due to the transfer of material to or from the surface (see Figure 7d). In this contrast, which has been observed over the same bias range as the other images reported here, the melamine hexagonal rings are enhanced with the bridging cyanuric acid molecules still clearly visible. We note that in Figure 7d two sites within the melamine rings appear occupied by adsorbed material. We therefore propose that this superstructure has the potential to be used to trap molecular species in a fashion similar to PTCDI−melamine networks,[18,19] and we are conducting further investigations into this.

Conclusions

In conclusion, we have shown that CA·M bimolecular arrays can be formed on the Au(111) surface with two distinct structures. The first, a honeycomb array is comparable with that observed previously on the Ag-Si(111)-($\sqrt{3} \times \sqrt{3}$)R30° surface.[20] The second larger superstructure is, thus far, unique to the Au(111) surface.

This work represents the second bimolecular network we have formed on both the Ag-Si(111)-($\sqrt{3} \times \sqrt{3}$)R30° and Au(111) surfaces, with comparable dimensions. By substituting cyanuric acid for PTCDI we have shown, on both surfaces, that we are able to form networks with reduced "pore" dimensions. This is highly relevant to noncovalently bonded surface templates[18,19,50−54] because we have been able to demonstrate that we can exhibit a degree of control of the dimensions of bimolecular networks through the choice of component molecules. We argue that our approach has the potential to form a wide range of template structures, with varying pore dimensions, which are able to trap molecules with subnanometer spatial organization on a wide range of surfaces.

Acknowledgment. We are grateful to the U.K. Engineering and Physical Sciences Research Council (EPSRC) for financial support under Grant GR/S97521/01.

References and Notes

(1) Lehn, J.-M. *Proc. Natl. Acad. Sci. U.S.A.* **2002**, *99*, 4763−4768.
(2) Balzani, V.; Credi, A.; Raymo, F. M.; Stoddart, J. F. *Angew. Chem., Int. Ed.* **2000**, *39*, 3348−3391.
(3) Reinhoudt, D. N.; Crego-Calama, M. *Science* **2002**, *295*, 2403−2407.
(4) Hecht, S. *Angew. Chem., Int. Ed.* **2003**, *42*, 24−26.
(5) De Feyter, S.; De Schryver, F. C. *Chem. Soc. Rev.* **2003**, *32*, 139−150.
(6) Böhringer, M.; Morgenstern, K.; Schneider, W.-D.; Berndt, R. *Angew. Chem., Int. Ed.* **1999**, *38*, 821−823.
(7) Furukawa, M.; Tanaka, H.; Kawai, T. *Surf. Sci.* **2000**, *445*, 1−10.
(8) Böhringer, M.; Morgenstern, K.; Schneider, W.-D.; Berndt, R.; Mauri, F.; De Vita, A.; Car, R. *Phys. Rev. Lett.* **1999**, *83*, 324−327.
(9) Barth, J. V.; Weckesser, J.; Cai, C.; Günter, P.; Bürgi, L.; Jeandupeux, O.; Kern, K. *Angew. Chem., Int. Ed.* **2000**, *39*, 1230−1234.
(10) Barth, J. V.; Weckesser, J.; Trimarchi, G.; Vladimirova, M.; De Vita, A.; Cai, C.; Brune, H.; Günter, P.; Kern, K. *J. Am. Chem. Soc.* **2002**, *124*, 7991−8000.
(11) Chen, Q.; Frankel, D. J.; Richardson, N. V. *Langmuir* **2002**, *18*, 3219−3225.
(12) Keeling, D. L.; Oxtoby, N. S.; Wilson, C.; Humphry, M. J.; Champness, N. R.; Beton, P. H. *Nano Lett.* **2003**, *3*, 9−12.
(13) Griessl, S.; Lackinger, M.; Edelwirth, M.; Hietschold, M.; Heckl, W. M. *Single Mol.* **2002**, *3*, 25−31.
(14) Dmitriev, A.; Lin, N.; Weckesser, J.; Barth, J. V.; Kern, K. *J. Phys. Chem. B* **2002**, *106*, 6907−6912.
(15) Tanaka, H.; Nakagawa, T.; Kawai, T. *Surf. Sci.* **1996**, *364*, L575−L579.
(16) Perdigão, L. M. A.; Staniec, P. A.; Champness, N. R.; Kelly, R. E. A.; Kantorovich, L. N.; Beton, P. H. *Phys. Rev. B* **2006**, *73*, 195423.
(17) Swarbrick, J. C.; Ma, J.; Theobald, J. A.; Oxtoby, N. S.; O'Shea, J. N.; Champness, N. R.; Beton, P. H. *J. Phys. Chem. B* **2005**, *109*, 12167−12174.
(18) Theobald, J. A.; Oxtoby, N. S.; Phillips, M. A.; Champness, N. R.; Beton, P. H. *Nature* **2003**, *424*, 1029−1031.
(19) Perdigão, L. M. A.; Perkins, E. W.; Ma, J.; Staniec, P. A.; Rogers, B. L.; Champness, N. R.; Beton, P. H. *J. Phys. Chem. B* **2006**, *110*, 12539−12542.
(20) Perdigão, L. M. A.; Champness, N. R.; Beton, P. H. *Chem. Commun.* **2006**, 538−540.
(21) Clair, S.; Pons, S.; Seitsonen, A. P.; Brune, H.; Kern, K.; Barth, J. V. *J. Phys. Chem. B* **2004**, *108*, 14585−14590.
(22) Vladimirova, M.; Trimarchi, G.; Baldereschi, A.; Weckesser, J.; Kern, K.; Barth, J. V.; De Vita, A. *Acta Mater.* **2004**, *52*, 1589−1595.
(23) Ma, J.; Rogers, B. L.; Humphry, M. J.; Ring, D. J.; Goretzki, G.; Champness, N. R.; Beton, P. H. *J. Phys. Chem. B* **2006**, *110*, 12207−12210.
(24) Yokoyama, T.; Yokoyama, S.; Kamikado, T.; Okuno, Y.; Mashiko, S. *Nature* **2001**, *413*, 619−621.
(25) De Wild, M.; Berner, S.; Suzuki, H.; Yanagi, H.; Schlettwein, D.; Ivan, S.; Baratoff, A.; Guentherodt, H.-J.; Jung, T. A. *ChemPhysChem* **2002**, *3*, 881−885.
(26) Berner, S.; Brunner, M.; Ramoino, L.; Suzuki, H.; Güntherodt, H.-J.; Jung, T. A. *Chem. Phys. Lett.* **2001**, *348*, 175.
(27) Lin, N.; Dmitriev, A.; Weckesser, J.; Barth, J. V.; Kern, K. *Angew. Chem., Int. Ed.* **2002**, *41*, 4779.
(28) Steiner, T. *Angew. Chem., Int. Ed.* **2002**, *41*, 48−76.
(29) Seto, C. T.; Whitesides, G. M. *J. Am. Chem. Soc.* **1990**, *112*, 6409−6411.
(30) Zerkowski, J. A.; Mathias, J. P.; Whitesides, G. M. *J. Am. Chem. Soc.* **1994**, *116*, 4305−4315.
(31) Zerkowski, J. A.; Seto, C. T.; Whitesides, G. M. *J. Am. Chem. Soc.* **1992**, *114*, 5473−5475.
(32) Mathias, J. P.; Simanek, E. E.; Zerkowski, J. A.; Seto, C. T.; Whitesides, G. M. *J. Am. Chem. Soc.* **1994**, *116*, 4316−4325.
(33) Mathias, J. P.; Simanek, E. E.; Whitesides, G. M. *J. Am. Chem. Soc.* **1994**, *116*, 4326−4340.
(34) Plater, M. J.; Sinclair, J. P.; Aiken, S.; Gelbrich, T.; Hursthouse, M. B. *Tetrahedron* **2004**, *60*, 6385−6394.
(35) Shao, X.-B.; Jiang, X.-K.; Zhu, S.-Z.; Li, Z.-T. *Tetrahedron* **2004**, *60*, 9155−9162.
(36) Mateos-Timoneda, M. A.; Kerckhoffs, J. M. C. A.; Crego-Calama, M.; Reinhoudt, D. N. *Angew. Chem., Int. Ed.* **2005**, *44*, 3248−3253.
(37) Mateos-Timoneda, M. A.; Crego-Calama, M.; Reinhoudt, D. N. *Chem. Soc. Rev.* **2004**, *33*, 363−372.
(38) Prins, L. J.; De Jong, F.; Timmerman, P.; Reinhoudt, D. N. *Nature* **2000**, *408*, 181−184.
(39) Barth, J. V.; Brune, H.; Ertl, G.; Behm, R. J. *Phys. Rev. B* **1990**, *42*, 9307−9318.
(40) Ordejón, P.; Artacho, E.; Soler, J. M. *Phys. Rev. B* **1996**, *53*, R10441−R10444.
(41) Soler, J. M.; Artacho, E.; Gale, J. D.; García, A.; Junquera, J.; Ordejón, P.; Sánchez-Portal, D. *J. Phys.: Condens. Matter* **2002**, *14*, 2745−2779.
(42) Perdew, J. P.; Burke, K.; Ernzerhof, M. *Phys. Rev. Lett.* **1996**, *77*, 3865−3868.
(43) Frey, J. A.; Leutwyler, S. *Chimia* **2005**, *59*, 511−516.

(44) Ireta, J.; Neugebauer, J.; Scheffler, M. *J. Phys. Chem. A* **2004**, *108*, 5692−5698.
(45) Troullier, N.; Martins, J. L. *Phys. Rev. B* **1991**, *43*, 1993−2006.
(46) Boys, S. F.; Bernardi, F. *Mol. Phys.* **1970**, *19*, 553−566.
(47) Wiebenga, E. H. *J. Am. Chem. Soc.* **1952**, *74*, 6156−6157.
(48) Cousson, A.; Nicolaï, B.; Fillaux, F. *Acta Crystallogr.* **2005**, *E61*, o222−o224.
(49) Ranganathan, A.; Pedireddi, V. R.; Rao, C. N. R. *J. Am. Chem. Soc.* **1999**, *121*, 1752−1753.
(50) Griessl, S. J. H.; Lackinger, M.; Jamitzky, F.; Markert, T.; Hietschold, M.; Heckl, W. M. *Langmuir* **2004**, *20*, 9403−9407.
(51) De Feyter, S.; Miura, A.; Yao, S.; Chen, Z.; Würthner, F.; Jonkheijm, P.; Schenning, A. P. H. J.; Meijer, E. W.; De Schryver, F. C. *Nano Lett.* **2005**, *5*, 77−81.
(52) Bonifazi, D.; Spillmann, H.; Kiebele, A.; De Wild, M.; Seiler, P.; Cheng, F.; Güntherodt, H.-J.; Jung, T.; Diederich, F. *Angew. Chem., Int. Ed.* **2004**, *43*, 4759−4763.
(53) Stepanow, S.; Lingenfelder, M.; Dmitriev, A.; Spillmann, H.; Delvigne, E.; Lin, N.; Deng, X.; Cai, C.; Barth, J. V.; Kern, K. *Nat. Mater.* **2004**, *3*, 229−233.
(54) Theobald, J. A.; Oxtoby, N. S.; Champness, N. R.; Beton, P. H.; Dennis, T. J. S. *Langmuir* **2005**, *21*, 2038−2041.